# Conversion of Light to Electricity by cis-X$_2$Bis(2,2'-bipyridyl-4,4'-dicarboxylate)ruthenium(II) Charge-Transfer Sensitizers (X = Cl⁻, Br⁻, I⁻, CN⁻, and SCN⁻) on Nanocrystalline TiO$_2$ Electrodes

**M. K. Nazeeruddin, A. Kay, I. Rodicio, R. Humphry-Baker, E. Müller, P. Liska, N. Vlachopoulos, and M. Grätzel***

*Contribution from the Institut de Chimie Physique, Ecole Polytechnique Fédérale de Lausanne, CH-1015 Lausanne, Switzerland*

**Abstract:** cis-X$_2$Bis(2,2'-bipyridyl-4,4'-dicarboxylate)ruthenium(II) complexes (X = Cl⁻, Br⁻, I⁻, CN⁻, and SCN⁻) were prepared and characterized with respct to their absorption, luminescence, and redox behavior. They act as efficient charge-transfer sensitizers for nanocrystalline TiO$_2$ films (thickness 8–12 $\mu$m) of very high internal surface area (roughness factor ca. 1000), prepared by sintering of 15–30-nm colloidal titania particles on a conducting glass support. The performance of cis-di(thiocyanato)bis(2,2'-bipyridyl-4,4'-dicarboxylate)ruthenium(II) (1) was found to be outstanding and is unmatched by any other known sensitizer. Nanocrystalline TiO$_2$ films coated with a monolayer of 1 harvest visible light very efficiently, their absorption threshold being around 800 nm. Conversion of incident photons into electric current is nearly quantitative over a large spectral range. These films were incorporated in a thin-layer regenerative solar cell equipped with a light-reflecting counter electrode. Short-circuit photocurrents exceeding 17 mA/cm$^2$ were obtained in simulated AM 1.5 sunlight using lithium iodide/triiodide in acetonitrile or acetonitrile/3-methyl-2-oxazolidinone mixtures as redox electrolyte. The open-circuit photovoltage was 0.38 V and increased to 0.72 V by treating the dye-covered film with 4-tert-butylpyridine. A solar-to-electric energy conversion efficiency of 10% was attained with this system. The effect of temperature on the power output and long-term stability of the dye was also investigated. For the first time, a device based on a simple molecular light absorber attains a conversion efficiency commensurate with that of conventional silicon-based photovoltaic cells.

## Introduction

While tris(2,2'-bipyridyl)ruthenium(II) and its homologues have been extensively investigated as redox sensitizers,[1] very little is known about the excited-state redox properties of the corresponding bis(2,2'-bipyridyl)ruthenium(II) analogoues. The reason for this is that the excited state of these compounds is often too short-lived to allow for occurrence of homogeneous bimolecular electron-transfer reactions.[2] However, heterogeneous charge-transfer processes might still be initiated with such sensitizers since they can take place on a very short time scale.[3] In a previous communication we have reported that cis-diaquabis(2,2'-bipyridyl-4,4'-dicarboxylate)ruthenium(II) (RuL$_2$(H$_2$O)$_2$) sensitizes wide band-gap semiconductors such as TiO$_2$ very efficiently over a broad spectral range in the visible.[4] A subsequent time-resolved luminescence study by Eichberger and Willig[3m] showed this effect to be due to ultrafast ($\tau < 7$ ps) electron injection from the excited state of the complex into the conduction band of the oxide occurring with a quantum yield near 100%. These important observations warrant further studies of the behavior of the relatively unexplored class of bis(2,2'-bipyridyl)ruthenium(II)-type redox sensitizers. Apart from their chemical stability and ease of interfacial charge exchange with semiconducting solids, the attractive feature of these complexes is their large visible light harvesting capacity which is superior to that of the widely studied tris(bipyridyl) Ru(II) analogues, making them a judicious choice for solar energy conversion devices.

The present paper reports the first systematic study of the luminescence, visible light absorption, electrochemical, and photoredox properties of bis(bipyridyl) Ru(II) complexes having the general formula cis-X$_2$bis(2,2'-bipyridyl-4,4'-dicarboxylate)-ruthenium(II), where X = Cl⁻, Br⁻, I⁻, CN⁻, and SCN⁻. Among these compounds, cis-di(thiocyanato)bis(2,2-bipyridyl-4,4'-dicarboxylate)ruthenium(II) (1) displays outstanding properties as a charge-transfer sensitizer, unmatched by any other dyestuff known so far. Its broad range of visible light absorption and relatively long-lived excited state render it an attractive sensitizer for homogeneous and heterogeneous redox reactions. In conjunction with the recently developed nanocrystalline colloidal TiO$_2$ films and iodide/triiodide electrolyte in an acetonitrile/3-methyl-2-oxazolidinone solvent mixture, this complex converts 10% of AM 1.5 solar radiation into electrical energy approaching the performance of polycrystalline silicon photovoltaic cells.

(1) (a) Gafney, H. D.; Adamson, A. W. *J. Am. Chem. Soc.* **1972**, *94*, 8238. (b) Whitten, D. G. *Acc. Chem. Res.* **1980**, *13*, 83. (c) Rubinstein, I.; Bard, A. J. *J. Am. Chem. Soc.* **1981**, *103*, 512. (d) Sutin, N. *Acc. Chem. Res.* **1982**, *13*, 273. (e) Adamson, A. W. *J. Chem. Educ.* **1983**, *60*, 803. (f) Meyer, T. J. *Prog. Inorg. Chem.* **1983**, *30*, 389. (g) Junis, A.; Balzani, V.; Barigelletti, F.; Campagna, S.; Balzer, P.; von Zelewsky, A. *Coord. Chem. Rev.* **1988**, *84*, 85. (h) Kalyanasundaram, K. *Photochemistry of Polypyridine and Porphyrin Complexes*; Academic Press: London, 1992 and references cited therein.

(2) (a) Klassen, D. M.; Crosby, G. A. *J. Chem. Phys.* **1968**, *48*, 1853. (b) Demas, J. N.; Crosby, G. A. *J. Am. Chem. Soc.* **1971**, *93*, 2841. (c) Krause, R. A.; Ballhausen, C. J. *Acta Chem. Scand. Ser. A* **1977**, *31*, 533. (d) Durham, B.; Wilson, S. R.; Hodgson, D. J.; Meyer, T. J. *J. Am. Chem. Soc.* **1980**, *102*, 600.

(3) (a) *Photoinduced Electron Transfer*; Fox, M. A., Chanon, M., Eds.; Elsevier: Amsterdam, 1988; Part A-4. (b) Grätzel, M. *Heteroigeneous Photochemical Electron Transfer*; For recent work on sensitized electron injection cf. also references cited hereafter. (c) Ryan, M. A.; Fitzgerald, E. C.; Spitler, M. T. *J. Phys. Chem.* **1989**, *93*, 6150. (d) Willig, F.; Eichberger, R.; Sundaresan, N. S.; Parkinson, B. A. *J. Am. Chem. Soc.* **1990**, *112*, 2702. (e) Amadelli, R.; Argazzi, R.; Bignozzi, C. A.; Scandola, F. *J. Am. Chem. Soc.* **1990**, *112*, 7099. (f) Nazeeruddin, M. K.; Liska, P.; Moser, J.; Vlachopoulos, N.; Grätzel, M. *Helv. Chim. Acta* **1990**, *73*, 1788. (g) Eichberger, R.; Willig, F. *Chem. Phys.* **1990**, *141*, 159. (h) Kim, Y. I.; Samer, S.; Hug, M. S.; Mallouk, Th. E. *J. Am. Chem. Soc.* **1991**, *113*, 9561. (i) Patrick, B.; Kamat, P. V. *J. Phys. Chem.* **1992**, *96*, 1423 and references cited therein.

(4) Liska, P.; Vlachopoulos, N.; Nazeeruddin, M. K.; Comte, P.; Grätzel, M. *J. Am. Chem. Soc.* **1988**, *110*, 3686.

*Conversion of Light to Electricity*

*J. Am. Chem. Soc., Vol. 115, No. 14, 1993* 6383

## Experimental Section

**Materials.** 3-Methyl-2-oxazolidinone (NMO) was synthesized by mixing 340 g (4 mol) of dimethylcarbonate (Fluka 39879) and 300 g (4 mols) of 2-methyl-aminoethanol (Fluka 65630) in a 1 L flask. After the catalyst, a solution of 2.3 g of sodium in 50 mL of methanol, was added, the flask was immediately fitted with a Vigreux column and immersed in cold water until the exothermic condensation reaction had ceased. The methanol was removed by distillation subsequently, and the remaining NMO was distilled under vacuum at ca. 1 Torr (bp = 90 °C). For further purification, the crude product was distilled again over calcium hydride (Fluka 21170). The purity of the solvent was confirmed by 200-MHz proton NMR. Chemical shifts against TMS were -$CH_3$, 2.9 ppm; -$CH_2$ (O-side), 4.32 ppm; -$CH_2$ (N-side), 3.58 ppm (coupling constant 8 Hz).

The ligand L = 2,2'-bipyridyl-4,4'-dicarboxylic acid (Alfa) and $RuCl_3 \cdot H_2O$ (Fluka) were commercial samples and used without further purification. All other materials were reagent grade and were used as received. $cis$-$Ru^{II}L_2Cl_2 \cdot 2H_2O$ and $cis$-$Ru^{II}L_2(H_2O)_2$ were synthesized using a previously described procedure.[4]

$cis$-Di(thiocyanato)-$N,N$-bis(2,2'-bipyridyl-4,4'-dicarboxylic acid)-ruthenium(II) dihydrate, $[RuL_2(NCS)_2] \cdot 2H_2O$ (**1**) was synthesized as follows: 283 mg (0.428 mmol) of $RuL_2Cl_2 \cdot 2H_2O$ was dissolved in 30 mL of DMF under reduced light. To this solution was added 20 mL of 0.1 M aqueous NaOH in order to deprotonate the carboxy groups. Sodium thiocyanate (350 mg, 4.52 mmol) was separately dissolved in 2 mL of $H_2O$ and subsequently added to the above solution. The reaction mixture was then heated to reflux for 6 h under nitrogen atmosphere, while magnetic stirring was maintained. After this time, the reaction mixture was allowed to cool, and the solvent was removed on a rotary evaporator. The resulting solid was dissolved in $H_2O$ and filtered through a sintered glass crucible. The pH of this filtrate was lowered to 2.5 by adding dilute $HClO_4$ or $CF_3SO_3H$, and the filtrate was placed in a refrigerator overnight. After reaching room temperature, the microcrystalline solid was isolated by suction filtration, washed well with $H_2O$/acetone–ether solution (1:10) followed by anhydrous diethyl ether, and air-dried for an hour (yield 80%). Elemental analysis for $C_{26}H_{16}N_6S_2O_8Ru \cdot 2H_2O$ gave (calculated values in parentheses): C, 41.65 (42.10); H, 2.86 (2.72); N, 11.26 (11.34).

Further structural characterization of **1** was carried out by IR spectroscopy using a DA 3.26 FTIR (BOMEM Inc., Quebec, Canada) or a Perkin-Elmer 6811 instrument. The high-resolution spectrum exhibits a doublet with peaks at 2126 and 2093 cm$^{-1}$, which is characteristic of the $cis$-configuration of the two thiocyanate ligands. Furthermore, the N-coordination of the thiocyanate group is confirmed by the presence of the $\nu$(C=S) resonance at 770 cm$^{-1}$. If the thiocyanate groups were coordinated to ruthenium through their sulfur atoms, a weak $\nu$(C=S) vibrational band around 700 cm$^{-1}$ would have appeared.[5] The fact that such a band was not observed excludes the presence of any significant amount of S-coordinated species in the product.

$cis$-Dicyanobis(2,2'-bipyridyl-4,4'-dicarboxylate)ruthenium(II) trihydrate was synthesized by dissolving 235 mg (3.6 mmol) of KCN in 10 mL of $H_2O$ and transferring it into a three-neck flask containing 30 mL of DMF. Subsequently, 500 mg (0.76 mmol) of $RuL_2Cl_2$ was introduced into the above solution. The reaction mixture was then heated to reflux under nitrogen for 5 h. During this period, the initially violet color of the solution changed to orange. After this time, the reaction mixture was allowed to cool and then filtered through a glass frit. The filtrate was evaporated to dryness on a rotatory evaporator, and the resulting solid was dissolved in $H_2O$ at pH 10. Upon addition of dilute $HClO_4$ or $CF_3SO_3H$ to the above solution, most of the complex precipitated as a neutral salt at pH 2–3. The orange solid was isolated by suction filtration, washed well with $H_2O$, ethyl–alcohol, and anhydrous diethylether, and air-dried for 1 h (yield 70%).

$cis$-Dibromo- and $cis$-diiodobis(2,2'-bipyridyl-4,4'-dicarboxylate)ruthenium(II) were synthesized by suspending 100 mg (0.148 mmol) of $RuL_2(H_2O)_2$ in 20 mL of $H_2O$ and stirring the mixture for 30 min in the dark. During this period, dilute NaOH solution (0.01 M) was added dropwise to dissolve the $RuL_2(H_2O)_2$. After dissolution of the $RuL_2(H_2O)_2$, the pH of the solution was lowered to 6–7, and the reaction mixture was filtered into a three-neck flask. An excess (100-fold) of KBr or KI was added to the above solution, which was then heated at reflux for 10 h under nitrogen atmosphere. This and subsequent manipulations
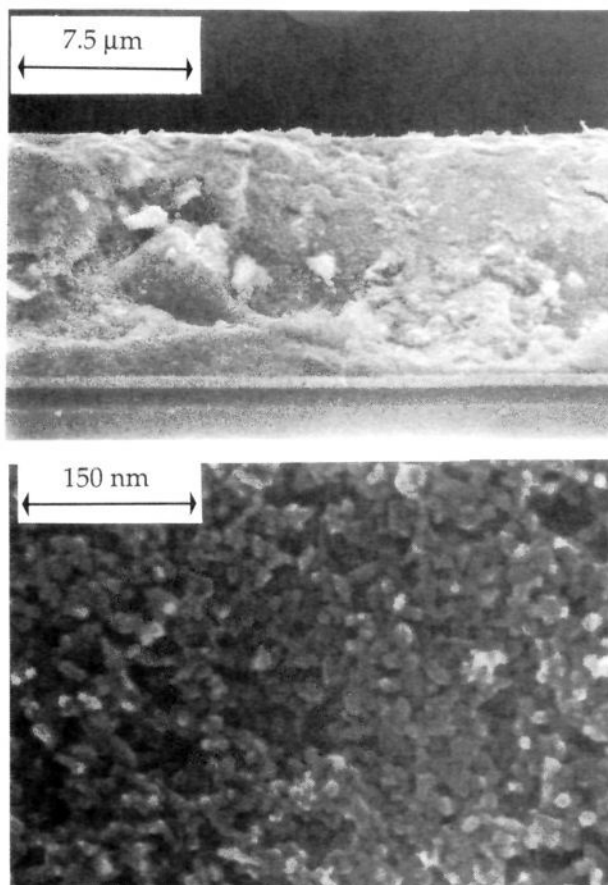




**Figure 1.** Scanning electron micrograph showing cross sections of the $TiO_2$ films deposited on conducting glass: top, low resolution and bottom, high resolution. Scales indicated on the photographs. Thickness of $TiO_2$ film was 10.4 $\mu$m; film was prepared by Method A.

were carried out under reduced light. After this period, the bromo and iodo complexes were isolated as a neutral salt at pH 2–3 by the addition of dilute $HClO_4$. The solid was collected on a glass frit by suction, washed thoroughly with $H_2O$, acetone–ether solution, and diethyl ether, and air-dried.

**Preparation of Nanocrystalline $TiO_2$ Films.** Nanocrystalline $TiO_2$ films were prepared by spreading a viscous dispersion of colloidal $TiO_2$ particles on a conducting glass support (Asahi TCO glass, fluorine-doped $SnO_2$ overlayer, transmission > 85% in the visible sheet resistance 7–8 $\Omega$/square) with heating under air for 30 min at 450 °C. Two methods of preparation of colloidal $TiO_2$ dispersions were employed. Method A followed the procedure described earlier,[6] except that autoclaving was performed at 230 or 240 °C instead of 200 °C. After the colloid was spread on the conducting glass support and calcined, a few monolayers of $TiO_2$ were electrodeposited[7] onto the colloidal $TiO_2$ film from an aqueous Ti(III) solution followed by renewed annealing at 450 °C. This treatment was found to improve significantly the short-circuit photocurrent as well as the open-circuit voltage of the solar cell. Figure 1 shows a cross section of such a $TiO_2$ film obtained by scanning electron microscopy at two different magnifications. The low resolution applied in Figure 1a confirms the presence of a three-layer structure, the lowest being the glass support followed by the 0.7-$\mu$m-thick fluorine-doped $SnO_2$ and the 10-$\mu$m-thick colloidal $TiO_2$ film. High resolution (Figure 1b) reveals the $TiO_2$ film to be composed of a three-dimensional network of interconnected particles having an average size of approximately 15 nm.

The second method for preparation of nanocrystalline films (Method B) employed commercial $TiO_2$ (P25, Degussa AG, Germany, a mixture of ca. 30% rutile and 70% anatase, BET surface area 55 m$^2$/g). This is produced by flame hydrolysis of $TiCl_4$ and consists of aggregated particles. Electron microscopy shows the mean size of primary particles to be about 25 nm. In order to break the aggregates into separate particles, the

(5) Nakamoto, K. *Infra Red and Raman Spectra of Inorganic and Coordination Compounds*; Wiley-Interscience: New York, 1970. Herber, R. H.; Nan, G.; Potenza, J. A.; Schugar, H. J.; Bino, A. *Inorg. Chem.* **1989**, *28*, 938.

(6) O'Regan, B.; Grätzel, M. *Nature (London)* **1991**, *353*, 737.
(7) Kavan, L.; O'Regan, B.; Kay, A. Grätzel, M. *J. Electroanal. Chem.* **1993**, *346*, 291.

**Table I.**   Absorption, Luminescence, and Electrochemical Properties of the [RuL₂X₂] Complexes

| complex[a] | abs max (nm)[b] ($E/10^4$ M⁻¹ cm⁻¹) | emission max (nm) at 298 K | emission max (nm) at 125 K | emission lifetime[d] $\tau$ (ns) at 298 K | emission lifetime[d] $\tau$ (ns) at 125 K | $\Phi$ (%) at 125 K | $E^\circ$ [e] |
|---|---|---|---|---|---|---|---|
| [RuL₂(NCS)₂] | 534 (1.42), 396 (1.40), 313 (3.12) | 755[b] | 718 | 50 | 960 | 0.40 | 0.85[f] |
| [RuL₂(CN)₂] | 493 (1.45), 365 (1.20), 310 (3.90) | 702 | 700 | 166 | 1123 | 1.5 | 1.16 |
| [RuL₂Cl₂] | 534 (0.96), 385 (1.01), 309 (4.13) | ~800[c] | 800 | | 105 | 0.074 | 0.57 |
| [RuL₂Br₂] | 530 (0.84), 382 (0.80), 309 (2.30) | ~800[c] | 750 | | 110 | 0.26 | 0.56 |
| [RuL₂I₂] | 536 (0.68), 384 (0.66), 310 (2.50) | ~800[c] | 755 | | 111 | 0.15 | 0.56 |
| [RuL₂(OH₂)₂] | 500 (1.19), 365 (1.09), 306 (4.90) | ~800[c] | 703 | | 165 | 0.30 | 0.58[g] |

[a] Isolated as neutral salts.  [b] Measured in C₂H₅OH; molar extinction coefficient values (±10%) are given in parentheses.  [c] Very weak and broad.  [d] Measured in ethanol/methanol (90/10 v/v).  [e] Electrolyte was tetrafluoroborate tetrabutylammonium salt/C₂H₄OH; all potentials reported vs SCE.  [f] Measured in CH₃CN.  [g] Measured in H₂O at pH 4.8.

powder (12 g) was ground in a porcelain mortar with a small amount of water (4 mL) containing acetylacetone (0.4 mL) to prevent reaggregation of the particles. Other stabilizers such as acids, bases, or TiO₂ chelatinbg agents were found to be suitable as well. After the powder had been dispersed by the high shear forces in the viscous paste, it was diluted by slow addition of water (16 mL) under continued grinding. Finally, a detergent (0.2 mL Triton X-100, Aldrich) was added to facilitate the spreading of the colloid on the substrate. The conducting TCO glass was covered on two parallel edges with adhesive tape (≈40-μm-thick) to control the thickness of the TiO₂ film and to provide noncoated areas for electrical contact. The colloid (5 μL/cm²) was applied to one of the free edges of the conducting glass and distributed with a glass rod sliding over the tape-covered edges. After air drying, the electrode was fired for 30 min at 450–550 °C in air. The resulting film thickness was 12 μm but can be varied by changing the colloid concentration or the adhesive tape thickness.

The performance of the film as a sensitized photoanode was improved by further deposition of TiO₂ from aqueous TiCl₄ solution. A 2 M TiCl₄ stock solution was prepared[7] at 0 °C to prevent precipitation of TiO₂ due to the highly exothermic hydrolysis reaction. This stock solution was freshly diluted with water to 0.2 M TiCl₄ and applied onto the electrode (50 μL/cm²). After being left overnight at room temperature in a closed chamber, the electrode was washed with distilled water. Immediately before being dipped into the dye solution, it was fired again for 30 min at 450–550 °C in air. Similarly to the electrodeposition from aqueous Ti(III) solution, this procedure results in the nucleation of nanometer-sized TiO₂ particles on the TiO₂ film, further increasing its active surface area. Furthermore, this treatment as well as the anodic deposition of TiO₂ from Ti(III) solution described above appears to lead to deposits having a very low impurity content. This is corroborated by the fact that the treatment becomes ineffective if the TiCl₄ solution is evaporated before firing instead of being washed off. Impurities in the TiCl₄, such as Fe³⁺, are not deposited by hydrolysis from the acidic TiCl₄ solution due to the higher solubility of iron oxide compared to TiO₂. By contrast, evaporation of the TiCl₄ solution results in the deposition of impurities. The P25 powder contains up to 100 ppm of Fe₂O₃, which is known to interfere with electron injection from the excited dye. The TiCl₄ treatment covers this rather impure core with a thin layer of highly pure TiO₂, improving the injection efficiency and the blocking character of the semiconductor–electrolyte junction.[7]

Coating of the TiO₂ surface with dye was carried out by soaking the film for at least 3 h in a 3 × 10⁻⁴ M solution of the ruthenium complex in dry ethanol. The dye coating was done immediately after the high-temperature annealing in order to avoid rehydration of the TiO₂ surface or capillary condensation of water vapor from ambient air inside the nanopores of the film. The presence of water in the pores decreases the injection efficiency of the dye. The electrode was dipped into the dye solution while it was still hot, i.e., its temperature was ca. 80 °C. After completion of the dye adsorption, the electrode was withdrawn from the solution under a stream of dry air or argon. It was stored in dry ethanol or immediately wetted with redox electrolyte solution for testing. The amount of adsorbed dye was determined by desorbing the dye from the TiO₂ surface into a solution of 10⁻⁴ M NaOH in ethanol and measuring its absorption spectrum.

**Methods.** A BAS-100 electrochemical analyzer (Bioanalytical Systems) was used to perform cyclic voltammetry in electrochemical cells with volumes of 5–20 mL. A three-electrode cell was comprised of a glassy carbon or Pt disk (3-mm-diameter embedded in Teflon (Du Pont)) working electrode and a platinum wire counter electrode. The reference electrode consisted of calomel in contact with 0.1 M LiCl in methanol. It was separated from the working electrode compartment by a bridge

containing the same electrolyte as the test solution, i.e., 0.1 M n-tetrabutylammonium perchlorate in acetonitrile or ethanol. All potentials indicated refer to the aqueous SCE electrode.

Photoelectrochemical experiments employed the dye sensitized TiO₂ film incorporated into a thin-layer sandwich-type solar cell. A light-reflecting counter electrode was employed, consisting of a conducting TCO glass onto which a 2-μm-thick Pt mirror had been deposited by sputtering. The counter electrode was placed directly on top of the dye-coated transparent TiO₂ film, supported by the conducting glass sheet. Both electrodes were clamped tightly together. A thin layer of electrolyte was attracted into the interelectrode space by capillary forces. The dye-coated TiO₂ film was illuminated through the conducting glass support. The conversion efficiencies reported are overall yields which are uncorrected for losses due to light absorption and reflection by the conducting glass support. An Oriel 450-W Xe lamp served as a light source in conjunction with a polycarbonate filter to remove ultraviolet radiation. The Schott 113 Tempax 3-mm filter was placed in the light beam to simulate AM 1.5-type solar emission.[8] Alternatively, an Oriel 81172 AM 1.5 solar simulator was used, giving practically identical results.

The emission spectra were measured on a Spex Fluorolog II equipped with a 450-W Xenon light source. The measured excitation and emission spectra were routinely corrected for the wavelength-dependent features using correction factors generated by a National Bureau of Standards 150-W halogen lamp. The emission detector was a Hamamatsu R2658 photomultiplier, which extended the corrected emission measurement over a region from 250 to 1000 nm. This was ideally suited to the red emission features of the ruthenium complexes used. All solutions were prepared by dissolving the appropriate amount of complex in the desired solvent to give typically a 2 × 10⁻⁵ M solution. The solutions were degassed by the freeze–pump–thaw method. Low-temperature measurements were carried out in an Oxford Instruments cryostat.

The emission lifetimes were measured by exciting the sample with an active mode-locked Nd YAG laser pulse, using the frequency-doubled line at 532 nm. The emission decay was followed on a Tektronix DSA 602A Digitizing Signal Analyzer. The digitized $xy$ data were subsequently analyzed and filtered to an exponential model. Sample concentrations were typically 1 × 10⁻⁴ M. Optical densities were taken from spectra recorded on a Cary 5 spectrophotometer.

## Results and Discussion

**Absorption, Luminescence, and Redox Properties.** Photophysical and electrochemical properties of cis-X₂bis(2,2'-bipyridyl-4,4'-dicarboxylic acid)ruthenium(II) complexes are listed in Table I. In agreement with the results for the unsubstituted cis-X₂-bis(2,2'-bipyridyl)Ru(II) analogues reported by Bryant et al.,[9] the carboxylated complexes exhibit two $\pi \rightarrow \pi^*$ intraligand transitions in the UV and two $t_2 \rightarrow \pi^*$ MLCT bands in the visible and near-UV. The visible $t_2 \rightarrow \pi^*$ absorption bands of RuL₂-(CN)₂ and RuL₂(NCS)₂ are more intense than those of the cis-dihalogeno and cis-diaqua derivatives. The absorption maximum

(8) The AM number characterizes the angle of incidence of solar light δ on the earth's surface: AM = 1/cos δ. An AM number of 1.5 corresponds to an angle of incidence of 37° and is used as a standard since it reflects well the annual average spectral distribution of solar light striking the earth at our lattitude. AM 1.5 solar emission was simulated by passing the output of the high-pressure 450-W xenon lamp through a 3-mm-thick Schott 113 interference filter, cf. also Solar Simulation for Research and Industry, Oriel Corp. catalogue.

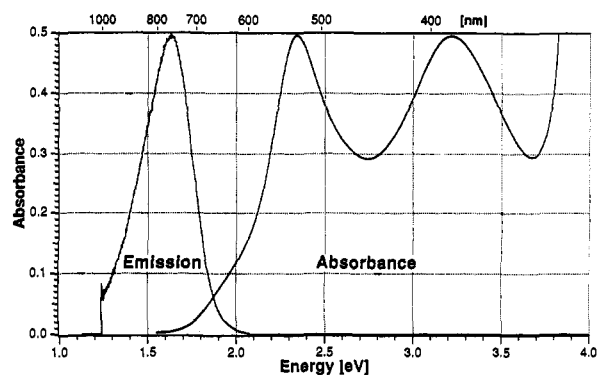(9) Bryant, G. M.; Fergusson, J. E.; Powell, H. K. J. *Aust. J. Chem.* **1971**, *24*, 257.

**Figure 2.** Absorption and emission spectra of a 3.5 × 10⁻⁵ M solution of **1** in ethanol. Optical pathlength was 1 cm. Excitation wavelength for the luminescence was 532 nm.

of RuL₂(NCS)₂ is red-shifted by 41 nm compared to that of RuL₂(CN)₂, which is advantageous for solar light harvesting.

The *cis*-dihalogeno- and *cis*-diaquo (X = Cl⁻, Br⁻ I⁻, and H₂O) derivatives display practically no emission at room temperature due to very short-lived excited states. A weak luminescence was observed at 125 K, the maximum being around 800 nm. In contrast to this behavior, RuL₂(CN)₂ and RuL₂(NCS)₂ luminesce at room temperature, their excited-state lifetimes in ethanol being 166 and 59 ns, respectively. The emission maximum of the former is 118 nm blue-shifted as compared to that of the latter. While Ru(bipy)₂(CN)₂ is known to luminesce in fluid solution,[18] the room temperature luminescence of *cis*-(SCN)₂bis(2,2-bipyridyl)-Ru(II) complexes has not been reported so far. The emission spectrum of the latter complex in ethanol is displayed in Figure 2, together with its visible and near-UV absorption features. The luminescence maximum is located at 755 nm, and the two MLCT absorption bands are centered at 534 and 389 nm, their extinction coefficients being 1.42 × 10⁴ and 1.40 × 10⁴ M⁻¹ cm⁻¹, respectively. From the intersection of the lowest energy absorption with the emission band, one derives[10] for the 0–0 transition energy of **1** a value of 1.75 eV.

Listed in Table I also are the reduction potentials of the sensitizers, ranging from 1.16 to 0.56 V vs SCE. RuL₂(CN)₂ exhibits the highest value, followed by RuL₂(NCS)₂ and the complexes with halide ligands. The standard potential for RuL₂-(NCS)₂ is 0.85 V (*vs* SCE) in acetonitrile, which is higher than $E_{1/2}$ = 0.67 V (*vs* saturated NaCl/calomel electrode) obtained[11] for the unsubstituted analogue Ru(bipy)₂(NCS)₂ in the same solvent. This is attributed to the electron-withdrawing properties of the carboxylate groups. Interestingly, there is no significant difference between the $E_{1/2}$ values of the three different halides, all of which are around 0.56 V. From their σ-donor strength one would have expected the chloride complex to have a lower potential than the iodide. The relatively high redox potentials of RuL₂-(CN)₂ and RuL₂(NCS)₂ are attributed to π back-bonding, i.e., electron donation from occupied Ru(II) t₂g orbitals to empty π* levels of the ligands. The CN group is a better π-acceptor than SCN, explaining why the former has the highest $E_{1/2}$ value and its absorption and emission spectra are blue-shifted with respect to the latter complex.

**Photocurrent Action Spectra of TiO₂ Films Coated with *cis*-X₂Bis(2,2′-bipyridyl-4,4′-dicarboxylate)ruthenium(II) Complexes.** Photocurrent action spectra obtained with the TiO₂ films

---

(10) Estimation of $E_{0-0}$ transition energy: the absorption and emission spectra were analyzed by Gaussian deconvolution methods (Igor, WaveMetrics Corporation, Lake Oswego, OR). This enabled surface area determination of the emission peak devoid of Raman and other instrumental artifacts. For the absorption spectra, Gaussian peaks could be assigned to the expected electronic CT transitions. The Gaussian peak for the low-energy S₀–T₁ transition was normalized to that of the emission maximum. The energy of the intersection of these two curves was taken as the value for $E_{0-0}$.

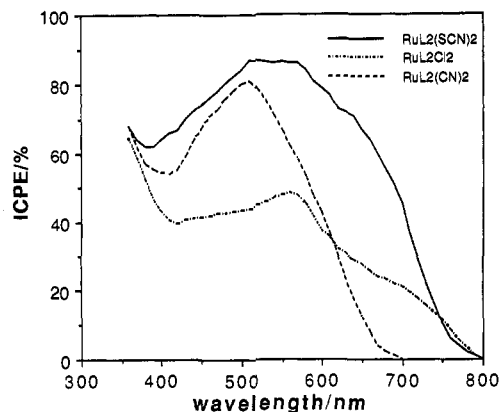(11) Durham, B.; Walsh, J. W.; Carter, Ch., Meyer, T. J. *Inorg. Chem.* **1980**, *19*, 860.



**Figure 3.** Photocurrent action spectra for nanocrystalline TiO₂ films coated with bis(2,2′-bipyridyl-4,4′-dicarboxylate)ruthenium(II) complexes. Films were prepared according to Method B. Spectra were obtained with the thin-layer cell containing a solution of 0.03 M I₂ and 0.3 M LiI in acetonitrile as electrolyte. The dye was excited through the conducting glass sheet serving as support for the TiO₂ film. The incident photon-to-current conversion efficiency is plotted as a function of excitation wavelength. The IPCE values are not corrected for the loss of light intensity due to absorption and reflection by the conducting glass support. The size of the working electrode was ca. 0.5 cm². The counter electrode was a conducting glass electrode covered with a transparent film of Pt. The cell was operated in the short-circuit mode.

coated with a monolayer of *cis*-X₂bis(2,2′-bipyridyl-4,4′-dicarboxylate)ruthenium(II) are shown in Figure 3. The incident monochromatic photon-to-current conversion efficiency (IPCE), defined as the number of electrons generated by light in the external circuit divided by the number of incident photons, is plotted as a function of excitation wavelength. This was obtained from the photocurrents by means of the following equation:

$$IPCE = \frac{[(1.25 \times 10^3) \times \text{photocurrent density } [\mu A/cm^2]]}{[\text{wavelength [nm]} \times \text{photon flux } [W/m^2]]} \quad (1)$$

The electrolyte used in this experiment was a solution of 0.3 M LiI and 0.03 M I₂ in acetonitrile. The photocurrent was obtained at short circuit where the TiO₂ film is poised to a potential of around 0.1 V measured against SCE. The intensity of the incident light was typically in the 0.05–1 mW/cm² range, and the photocurrent obtained was 15–300 μA/cm². The TiO₂ film was illuminated from the front side through the conducting glass support. The yields reported are uncorrected for the absorption and scattering of incident light (ca. 10–15%) by the glass. While bare TiO₂ films due to their large band gap give practically no photocurrents above 440 nm,[6] the response of the electrodes coated with *cis*-X₂bis(2,2′-bipyridyl-4,4′-dicarboxylate)ruthenium(II) is excellent. Particularly impressive is the performance of RuL₂-(NCS)₂, for which the IPCE values exceed 80% in the wavelength range between 480 and 600 nm, attaining a plateau of 85–90% between 510 and 570 nm. Taking the losses due to the conducting glass support into account, this implies that the conversion of photon flux impinging onto the film into electrical current in the external circuit is practically quantitative in this wavelength domain.

In order to rationalize these observations, the monochromatic current yield (or incident monochromatic photon-to-current conversion efficiency) is expressed in terms of the light harvesting efficiency (LHE), the quantum yield of charge injection ($\phi_{inj}$), and the efficiency of collecting the injected charge at the back contact ($\eta_c$)

$$IPCE(\lambda) = LHE(\lambda) \, \phi_{inj}\eta_c \quad (2)$$

The fact that the value of IPCE is practically 100% between 510 and 570 nm implies that all three factors in eq 2 must also be

100% within this wavelength range. In the following we analyze these three terms separately.

The light harvesting efficiency is given by

$$LHE(\lambda) = 1 - 10^{-\Gamma\sigma(\lambda)} \tag{3}$$

where $\Gamma$ is the number of moles of sensitizer per square centimeter of projected surface area of the film and $\sigma$ is the absorption cross section in units of $cm^2/mol$ obtained from the decadic extinction coefficient (units of $M^{-1}\,cm^{-1}$) by multiplication with $1000\,cm^3/L$. Because the surface concentration of $RuL_2(NCS)_2$ is around $1.3 \times 10^{-7}\,mol/cm^2$ and $\sigma$ is $1.42 \times 10^7\,cm^2/mol$, the light harvesting efficiency is 98% at the absorption maximum of the sensitizer and still 88% at the wavelength of half maximum height. This insures efficient photon capture by $RuL_2(NCS)_2$ in a broad spectral range in the visible. It also explains why the action spectrum for $RuL_2(NCS)_2$ in Figure 3 is much broader than its absorption feature in Figure 2. The decline of the ICPE above 600 nm toward the red is caused by the decrease in the extinction coefficient of 1. On the other hand, the drop in the ICPE between 500 and 400 nm is mainly due to the filtering of light by the triiodide anions.

The quantum yield of charge injection is given by

$$\phi_{inj} = k_{inj}/(\tau^{-1} + k_{inj}) \tag{4}$$

where $k_{inj}$ is the rate constant for electron injection and $\tau$ is the excited-state lifetime in the absence of injection. It can be assumed that both $k_{inj}$ and $\tau$ are wavelength independent. Using $\tau = 59$ ns from Table I and $k_{inj} > 1.4 \times 10^{11}\,s^{-1}$ determined by Eichberger and Willig[3s] for $Ru^{II}L_2(H_2O)_2$, one obtains $\phi_{inj} > 99.9\%$. Thus, photons absorbed by the sensitizer are quantitatively converted to conduction band electrons.

The fraction of injected charges that is able to reach the back contact is given by the factor $\eta_c$ in eq 2. Recent time-resolved laser photolysis experiments have shown[12] that the injected electrons can percolate without significant loss through the network of interconnected particles present in the nanocrystalline $TiO_2$ film. The back-reaction is relatively slow, i.e., in the $10^{-7}$–$10^{-5}$-s range, and it may be further retarded by the depletion layer field present at the semiconductor surface. It should be appreciated, however, that due to the very small size of the $TiO_2$ particles, the potential barrier at the solid-electrolyte junction is expected to be relatively small.[12] This contrasts with conventional photovoltaic or photoelectrochemical devices where a significant junction potential is required to separate the charge carriers produced by light excitation. In the newly developed nanocrystalline semiconductor films, the importance of this potential barrier is diminished. Charge carriers recombination is here sufficiently slow, even in the absence of an electric field, that it can be intercepted efficiently by the reaction of the electron donor, e.g., iodide, with the oxidized dye. The iodide reduces the Ru(III) complex produced at the photoanode, regenerating the original Ru(II) oxidation state. The iodide is oxidized to triiodide in this process. The latter may be reduced back to iodide by conduction band electrons, eq 5, providing a second channel for charge recombination. However, this process is very slow under reverse bias, as indicated by the absence of any significant dark current. This explains why the electrons can percolate through the nanostructured film without significant loss though recombination, resulting in near quantitative charge collection. High charge separation and collection yields have also been observed with similar nanocrystalline $TiO_2$ layers excited via band gap excitation, and a model for charge carrier migration within the film has been proposed.[13] In the latter case, recombination was intercepted by hole scavenging with thiocyanate. Since in nanocrystalline $TiO_2$
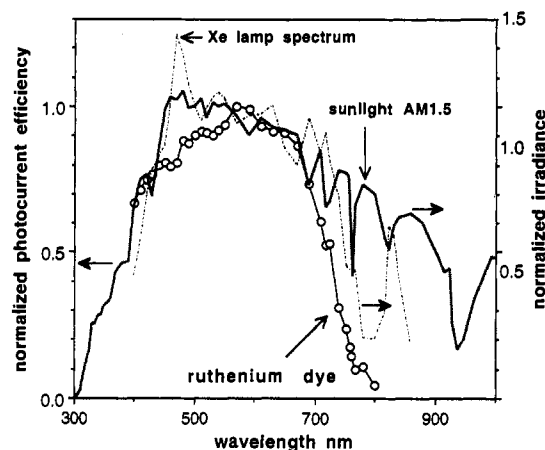


**Figure 4.** Spectral overlap of AM 1.5 solar emission with the photocurrent action spectrum obtained for complex **1**.

films the distance the hole has to travel to reach the semiconductor-electrolyte interface is only a few nanometers, the diffusion time is at most a few picoseconds. As a result, the hole scavenging at the surface competes very efficiently with charge carrier recombination in analogy to the present sensitization experiments.

The tail of the action spectrum of $RuL_2(NCS)_2$ in Figure 3 extends well into the red, the IPCE being still as high as 45% at 700 nm. The photocurrent onset threshold is close to 800 nm, corresponding to a 0–0 transition energy of 1.55 eV for the adsorbed sensitizer. This is 0.2 eV smaller than the $E_{0-0}$ value for the free complex, indicating that the charge-transfer transition of **1** is red-shifted upon adsorption at the surface of $TiO_2$. A similar red shift in the photocurrent action spectrum has also been observed for the tris(bipyridyl) complex $Ru^{II}(bipy)_2L$, and the effect has been interpreted in terms of an increase in the delocalization of the $\pi$ orbital of the bipyridine ligand upon adsorption of the complex at the surface of $TiO_2$.[14] The interaction of the carboxylate group with surface Ti ions is likely to lead to the formation of C–O–Ti bonds. The carboxylate serves, therefore, as an interlocking group enhancing electronic coupling between the $\pi^*$ orbitals of the 2,2'-bipy ligand and the Ti(3d) orbital manifold of the semiconductor. This coupling is rendered efficient by the presence of $\pi$ electrons in the bridging group leading to increased delocalization of the $\pi^*$ level of the 2,2'-bipy ligand. The energy of the $\pi^*$ level is decreased by this delocalization, which explains the observed red shift in the photocurrent action spectrum. Similar shifts were observed for the other complexes investigated. Thus, in Figure 3 the photocurrent action spectrum of $Ru(L)_2(CN)_2$ has a maximum at 515 nm, while the absorption peak in solution is centered at 493 nm. Similarly, for $RuL_2Cl_2$ the absorption maximum in solution is at 534 nm, while that of the photocurrent action spectrum is at 566 nm. The other halide complexes exhibit action spectra resembling closely that of $RuL_2Cl_2$, albeit with lower conversion yields. For clarity of presentation, these data were omitted from Figure 3.

The photocurrent response of the cell to red light can be further improved by applying light-management strategies known from amorphous silicon solar cell technology.[15] The approach is to randomize the incident light by using nanoparticles for film formation that are large enough to scatter visible light in conjunction with a light-reflecting counter electrode. Complete randomization would result in a $4n^2$-times increased optical absorption of the film in the tail region of the dye spectrum ($n$ is the refractive index of the dye-loaded film in the same wavelength region). Figure 4 shows the action spectrum of a $RuL_2(NCS)_2$ coated $TiO_2$ film (thickness of 8 $\mu m$) obtained with a light-reflecting counter electrode. The effect of the light

(12) O'Regan, B.; Moser, J.; Anderson, M.; Grätzel, M. *J. Phys. Chem.* **1990**, *94*, 8720.

(13) Hagfeldt, A.; Björksten, U.; Lindquist, S.-E. *Sol. Energy Mater. Sol. Cells* **1992**, *27*, 293.

(14) Gulino, D. A.; Drickamer, H. G. *J. Phys. Chem.* **1984**, *88*, 1173.

(15) Deckmann, H.; Yablonovitch, E. *Appl. Phys. Lett.* **1983**, *42*(11), 968.

*Conversion of Light to Electricity*

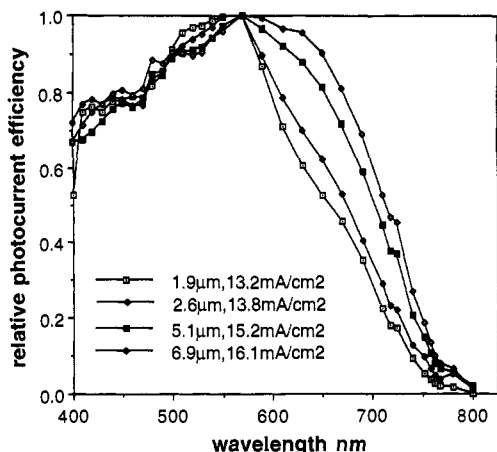*J. Am. Chem. Soc., Vol. 115, No. 14, 1993* 6387



**Figure 5.** Effect of layer thickness on the photocurrent action spectra for nanocrystalline TiO₂ films sensitized by **1**. Conditions and film preparation methods as in Figure 2.

management is to increase the photocurrent yields in the 600–800-nm region, where the absorption of the dye-coated TiO₂ film decreases sharply.

Also shown in Figure 4 is the AM 1.5 solar emission spectrum and the spectral distribution of the Xe lamp light used for solar simulation. The global 1.5 spectral solar irradiance data set of Hulstrom et al.,[16] referring to a sun-facing surface tilted 37° from the horizontal, was used as a standard. The total intensity is 96.4 mW/cm². The overlap integral was calculated using the IPCE values from Figure 4 and assuming a constant IPCE value of 0.7 between 310 and 390 nm, the value at 530 nm being 0.85 ± 0.1. The calculated photocurrent density is 16.6 ± 1.9 mA/cm². The photocurrent obtained with the same film at 96.4 mW/cm² of simulated solar intensity was 18.2 mA/cm². The difference may arise from a spectral mismatch between the simulated and true AM 1.5 sunlight. In order to check this possibility, the cell performance was measured under direct sunlight in March at noon on the roof of this institute, where the spectral distribution was close to AM 1.5. The short-circuit current was similar to the value obtained with the simulator, indicating that the spectral mismatch is small.

The calculated short-circuit photocurrent may be underestimated since it is difficult to determine precisely the IPCE values in the wavelength region above 700 nm. The photocurrents are very small due to the low monochromatic output in this wavelength region. The level of photoconductivity induced by red light in the nanocrystalline film is insufficient to ascertain collection of all the photoelectrons injected by the excited dye.[17] Because the extinction coefficient of the dye is small in the red, charge carriers are generated uniformly over the whole film thickness. Thus, a large fraction of the photoinjected electrons have to diffuse over a long distance within the nanocrystalline film before reaching the current collector. Due to electron trapping and insufficient conductivity of the nanocrystalline TiO₂ film, part of the charge carriers generated away from the conducting glass are lost, decreasing the IPCE value. The collection efficiency becomes close to 100% under sunlight exposure, where charge carrier trapping and conduction problems do not arise.

The action spectra obtained with RuL₂(NCS)₂ are strongly influenced by the TiO₂ film thickness and morphology. Figure 5 shows results for four different films whose thickness varied from 1.9 to 6.9 μm. For ease of inspection, the action spectra were normalized to a common IPCE value of 1 at their maximum at 570 nm. Increasing the film thickness improves the harvesting of red light, increasing the short-circuit photocurrents. The values
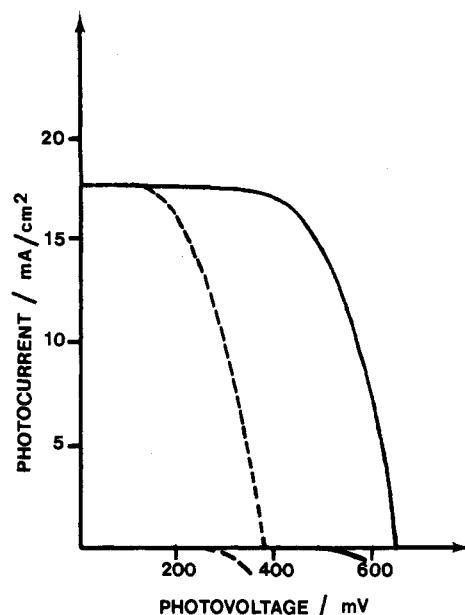


**Figure 6.** Photocurrent–voltage charcteristics of a cell based on a colloidal TiO₂ film (prepared via Method A) sensitized by **1**. The film, supported on a conducting glass sheet, was used in a sandwich-type configuration. The size of the dye-coated TiO₂ photoanode was 0.5 cm². A light-reflecting counter electrode consisting of conducting glass coated with a 2.5-μm-thick layer of Pt was placed directly on top of the working electrode. A thin layer of redox electrolyte is attracted into the intraelectrode space through capillary forces. The onset of the dark current is also shown. Dashed line: untreated electrode; solid line: same electrode dipped for 15 min in 4-*tert*-butylpyridine after dye coating. Conditions: electrolyte, 0.3 M LiI + 0.03 M I₂ in acetonitrile, room temperature, light intensity 87 mW/cm², AM 1.5 spectral irradiance.

inserted in the figure were calculated as before from the overlap integral of the current action spectra with the AM 1.5 solar emission with IPCE = 0.86 at 530 nm and 96.4 mW/cm² incident light intensity. Because the short-circuit photocurrent observed with dye-sensitized TiO₂ depends on film thickness and morphology, the photovoltaic performance is strongly affected by the method applied for the fabrication of the nanocrystalline layers. It is not surprising, therefore, that large variations in the short-circuit current can be observed between different electrode preparations. Thus Knödler et al.[18] and Hagfeldt et al.[19] have recently obtained very high short-circuit currents exceeding 20 mA/cm² with RuL₂(NCS)₂ under simulated AM 1.5 solar light by using screen printing or spraying procedures to fabricate the TiO₂ films.

**Current–Voltage Characteristics and Conversion Yields of Regenerative Cells.** Figure 6 shows the current–voltage characteristics obtained with a thin-layer sandwich-type cell under illumination by simulated AM 1.5 solar light. The counter electrode was placed directly on top of the RuL₂(NCS)₂-coated TiO₂ film, the electrolyte (a solution of 0.3 M LiI and 0.03 M I₂ in acetonitrile) being attracted into the interelectrode space by capillary forces. In order to increase the light harvesting capacity of the device, a 2-μm-thick Pt mirror was sputtered onto the TCO counter electrode. Apart from reflecting the light that passes through the film, the platinum serves to catalyze the cathodic reduction of triiodide at the conducting glass. The two photo-current–voltage curves in Figure 6 refer to the same RuL₂(NCS)₂-coated TiO₂ film, the solid curve being obtained after the RuL₂(NCS)₂-coated electrode was dipped for 15 min in 4-*tert*-butylpyridine, The exposure of 4-*tert*-butylpyridine improves

(16) Hulstrom, R.; Bird, R.; Riordan, C. *Sol. Cells* **1985**, *15*, 365.

(17) Our recent work carried out after completion of this study confirmed that the IPCE values in the red region (λ > 700 nm) decrease if the incident monochromatic light intensity is below 0.2 mW/cm².

(18) Hagfeldt, A.; Didriksson, B.; Palmquist, T.; Lindström, H.; Södergren, S.; Rensmo, H.; Lindquist, S.-E. *Sol. Energy Mater. Sol. Cells*, in press. We thank Dr. Lindquist for informing us on these results prior to publication.

(19) Knödler, R.; Sopka, J.; Harbach, F.; Grünling, H. W. *Sol. Energy Mater. Sol. Cells*, in press. We thank Dr. Knödler for communicating these results to us.

dramatically the fill factor (ff) and open-circuit voltage ($V_{oc}$) of the device without affecting the short-circuit photocurrent ($i_{sc}$) in a significant fashion. Thus the untreated electrode gave $i_{sc}$ = 17.8 mA/cm$^2$, $V_{oc}$ = 0.38 V, and ff = 0.48, corresponding to an overall conversion efficiency ($\eta$) of 37%. After the electrode is dipped in 4-*tert*-butylpyridine, $V_{oc}$ increases to 0.66 V, ff to 0.63, and $\eta$ to 8.5%.

The increase in the open-circuit voltage and fill factor by 4-*tert*-butylpyridine is due to the suppression of the dark current at the semiconductor electrolyte junction. The dark current arises from the reduction of triiodide by conduction band electrons:

$$I_3^- + 2e_{cb}^-(TiO_2) \rightarrow 3I^- \qquad (5)$$
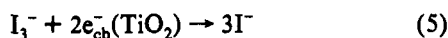
which occurs despite the fact that the TiO$_2$ surface is covered by a monolayer of RuL$_2$(NCS)$_2$. The triiodide, due to its relatively small size, either crosses the dye layer or has access to nanometer-sized pores into which the RuL$_2$(NCS)$_2$ cannot penetrate, i.e., where the surface of TiO$_2$ is bare and exposed to redox electrolyte. The effect of 4-*tert*-butylpyridine is to decrease the rate of the reduction of triiodide. This is clearly visible in Figure 6, where the onset of the dark current is shifted by ca. 200 mV upon pyridine treatment. The decrease in the rate constants for triiodide reduction ($k_{et}$) should lead to an increase in the open-circuit voltage of the cell. For regenerative photoelectrochemical systems, the following relation holds:[20,21]

$$V_{oc} = \left(\frac{kT}{e}\right) \ln \left(\frac{I_{inj}}{n_{cb}k_{et}[I_3^-]}\right) \qquad (6)$$

where $I_{inj}$ is the flux of charge resulting from sensitized injection and $n_{cb}$ is the concentration of electrons at the TiO$_2$ surface. The open-circuit voltage increases from 0.38 to 0.66 V upon treating the TiO$_2$ surface with 4-*tert*-butylpyridine, corresponding to a 5.5 × 10$^4$-fold decrease in the rate constant for triiodide reduction. Apparently, adsorption of 4-*tert*-butylpyridine at the TiO$_2$ surface has a dramatic effect on the rate of interfacial electron transfer from the conduction band of TiO$_2$ to triiodide. This is rationalized in terms of adsorption of 4-*tert*-butylpyridine at the TiO$_2$ surface blocking surface states that are active as intermediates in the heterogeneous charge transfer. Presumably, these sites are represented by Ti(IV) ions on the surface, which, due to their Lewis acidity, are prone to interact with the pyridine derivative. The importance of such surface states in mediating interfacial charge-transfer processes at the TiO$_2$/solution boundary has recently been established by laser photolysis studies[22] with colloidal TiO$_2$.

The short-circuit currents increase linearly with light intensity up to about 1 sun, and this is illustrated in Figure 7. This linearity shows that the photocurrent is not limited by diffusion of the iodide or triiodide ions within the nanocrystalline film up to current densities of at least 20 mA/cm$^2$.

A further improvement in conversion efficiency was obtained by using a mixture (90/10, v/v) of acetonitrile and NMO as a solvent for the iodide/triiodide electrolyte. NMO is suitable as a cosolvent on the basis of its high polarity, high boiling point, high solvent donor number, and very good stability.[23] The effect of NMO addition to the electrolyte is to increase further the open-circuit voltage, and this overcompensates for a small loss in short-circuit current. Results are presented in Figure 8 and Table II. The open-circuit voltage increases with light intensity, while the fill factor decreases due to Ohmic losses in the conducting glass support. As a consequence, the overall conversion efficiencies
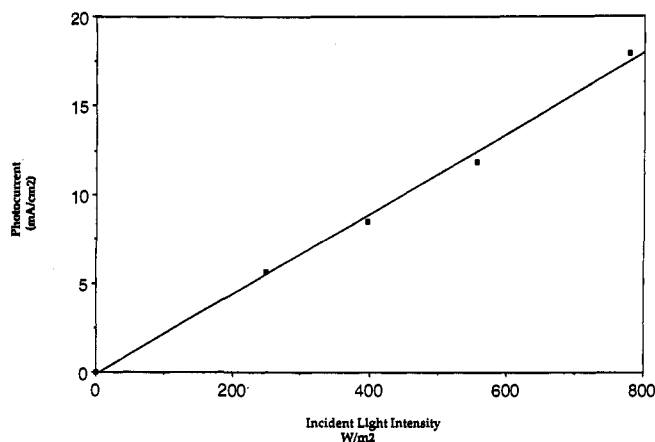
(20) Rosenblut, M. L.; Lewis, N. S. *J. Phys. Chem.* **1989**, *93*, 3735.

(21) Kumer, A.; Santangelo, P. G.; Lewis, N. S. *J. Phys. Chem.* **1992**, *96*, 835.

(22) (a) Moser, J.; Punchihewa, S.; Infelta, P. P.; Grätzel, M. *Langmuir* **1991**, *7*, 3012. (b) Frei, H.; Fitzmaurice, D. J.; Grätzel, M. *Ibid.* **1990**, *6*, 198.

(23) (a) Huffman, H. L.; Sears, P. G. *J. Solution Chem.* **1972**, *1*, 187. (b) Kelly, M. J.; Heineman, W. R. *J. Electroanal. Chem.* **1988**, *248*, 441.



**Figure 7.** Effect of light intensity on the short-circuit photocurrent of the cell. Conditions: electrolyte as in Figure 5, TiO$_2$ surface treated with 4-*tert*-butylpyridine before being wetted with electrolyte, room temperature, AM 1.5 spectral irradiance.
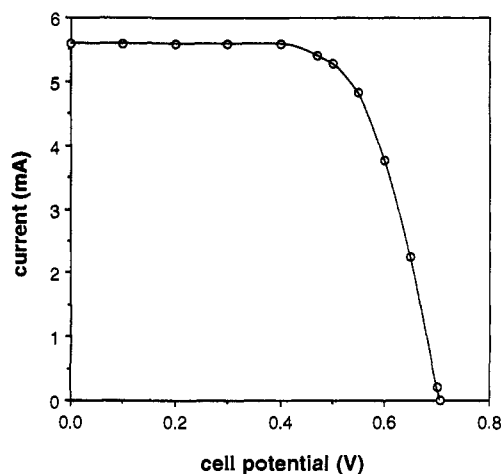


**Figure 8.** Photocurrent–voltage characteristics of nanocrystalline titanium dioxide cell. Conditions as in Figure 5 except that a mixture of acetonitrile and 3-methyl-2-oxazolidinone (90/10, v/v) was used as a solvent for the iodine/iodide redox electrolyte. Performance parameters are listed in Table II. The films were dipped for 15 min in *tert*-butylpyridine before being wetted with electrolyte. The amount of adsorbed sensitizer was 1.3 × 10$^{-7}$ mol/cm$^2$. Size of TiO$_2$ electrode was 0.31 cm$^2$.

**Table II.** Performance Characteristics of Photovoltaic Cells Based on Nanocrystalline TiO$_2$ Films Sensitized by *cis*-Di(thiocyanato)bis(2,2′-bipyridyl-4,4′-dicarboxylate)ruthenium(II)

| light intensity[a] (mW/cm$^2$) | $i_{sc}$ (mA/cm$^2$) | $V_{oc}$ (mV) | $ff$ | $\eta^b$ (%) |
|---|---|---|---|---|
| 24.1[c] | 5.0 | 640 | 0.76 | 10.4 |
| 38.2[c] | 7.9 | 660 | 0.76 | 10.4 |
| 55.6[c] | 11.5 | 670 | 0.74 | 10.3 |
| 96.0[d] | 18.2 | 720 | 0.73 | 10.0 |

[a] Simulated AM 1.5 solar radiation. [b] Overall light-to-electric energy conversion efficiency. [c] Electrolyte: mixture of acetonitrile/NMO (90/10, v/v) [Li] = 0.3 M, [I$_2$] = 0.03 M. [d] TiO$_2$ film employed was the same as in Figure 4. The current–voltage curve is shown in Figure 8.

remain close to 10% within light intensities ranging from 24.1 to 96 mW/cm$^2$, the highest yield being observed at 38.2 mW/cm$^2$ where $\eta$ = 10.4%.

**Temperature Effects on Cell Performance.** A double-wall cell connected to a Haake H6 thermostat was used in these experiments. Incident light intensity was 96.0 mW/cm$^2$. The electrolyte was 0.5 M LiI and 0.04 M I$_2$ in acetonitrile/NMO (70/30, v/v). The NMO content of the solvent was higher than in the preceding experiments to allow for extension of the upper limit of the accessible temperature range. Results are shown in
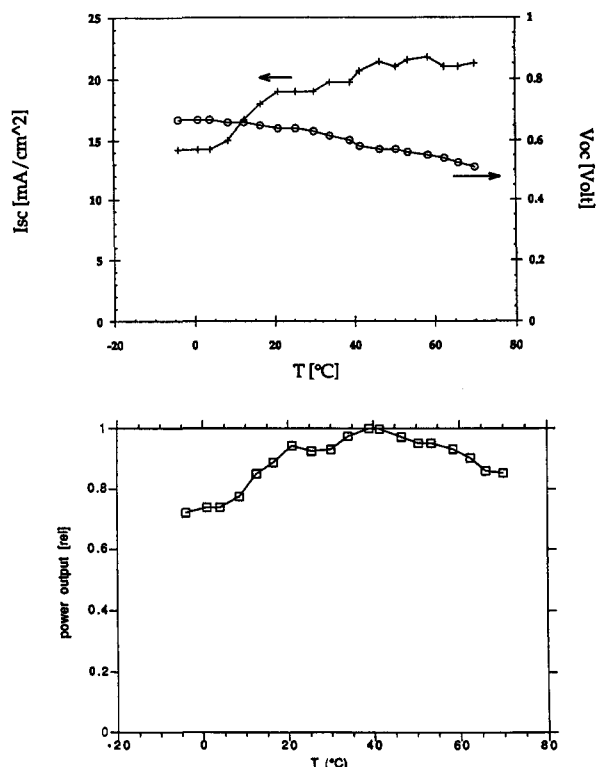
**Figure 9.** Effect of temperature on the performance characteristics of the cell. Electrolyte: 0.5 M LiI + 0.04 M $I_2$ in a mixture (60/40, v/v) of NMO/acetonitrile. $TiO_2$ surface treated with 4-*tert*-butylpyridine after dye coating.

Figure 9. Increasing the temperature from $-5$ to 70 °C decreases $V_{oc}$ from 0.67 to 0.51 V, while the $i_{sc}$ rises from 14.2 to 21.2 mA/cm$^2$. The fill factor shows practically no change with temperature for the electrolyte employed. However, with solvents such as propylene carbonate which have a relatively high viscosity, the fill factor was found to increase with temperature. The voltage decrease is traceable to an augmentation of the dark current with temperature. An increased dark current implies a higher value for the rate constant of triiodide reduction, which, according to eq 6, leads to a lower value for $V_{oc}$.

The changes in the short-circuit photocurrent occur mainly below 20 °C. In this temperature domain, $i_{sc}$ decreases due to increased electrolyte viscosity, leading to mass-transfer limitation of triiodide reduction at the counter electrode. This is corroborated by the finding that $i_{sc}$ is practically temperature independent if the cell is illuminated with light of lower intensity, e.g., 10 mW/cm$^2$. The important information inferred from the latter result is that the photon-to-current conversion efficiencies are not affected by temperature within the range investigated. Apart from the dark current, there are no discernable thermal effects on the performance of the photoelectrode. In particular, it appears that the rate of sensitized charge injection is independent of temperature, which is in keeping with it being a quantum mechanical tunnelling process.[24]

The effect of temperature on the total power output of the cell is relatively small due to the various compensating factors contributing to cell performance. The optimum temperature in Figure 9 is at 40 °C.

**Long-Term Stability of the Sensitizer.** One of the most striking features of **1** it its excellent stability under long-term irradiation. Since this is a vital parameter for sustained cell operation, we have started detailed studies with this promising sensitizer and report here preliminary results. To facilitate the analysis, visible light was used as in previous stability studies with a trimeric

ruthenium complex.[6] Band-gap excitation of the $TiO_2$ was avoided by inserting a 420-nm cut-off filter or a 1-mm-thick polycarbonate sheet in the light beam. Polycarbonate absorbs UV radiation below 390 nm. Band-gap excitation is not entirely suppressed by the latter type of filter, especially for films produced from Method B colloids since they contain 30% rutile. The band gap of rutile is 3 eV, as compared to 3.2 eV for anatase, corresponding to a fundamental absorption edge of 413 and 388 nm, respectively. Therefore, the UV effects[25] are greatly attenuated but not completely eliminated by the polycarbonate. In order to scrutinize the stability of the sensitizer, several thin-layer cells have been subjected to long-term irradiation. Solutions of LiI/LiI$_3$ in pure NMO or propylene carbonate were used as an electrolyte.[26] They have been continuously illuminated with the light output from a 450-W overhead projector or a 150-W tungsten–halogen lamp filtered through polycarbonate in most cases. Operation temperature has been around 50 °C. The longest continuous exposure time has been 10 months so far. All cells illuminated through the polycarbonate filters showed an initial decline in photocurrent which typically was between 20 to 30%. The decrease is smaller if band gap excitation of $TiO_2$ is strictly avoided, e.g., by use of anatase colloid in conjunction with the 420-nm cut-off filter. Hence, it is attributed to absorption of residual UV light passing through the polycarbonate sheet[25] and to water contamination.[26]

There is a change in the cell performance after exposing the dye-coated films to the electrolyte, even if the cell is kept in the dark. Usually the short-circuit photocurrent decreases during the first day by about 10%, while the open circuit voltage and the fill factor increase. The overall AM 1.5 conversion efficiency increases or remains constant during this phase. These dark effects are attributed to the electronic and chemical equilibration of the dye-loaded $TiO_2$ with the electrolyte.[26] These effects are caused principally by water uptake from ambient air. Their extent depends on the composition of the liquid employed. Following the initial phase, which is terminated within 2–20 days, the photocurrent has been stable over the remaining period, lasting for more than 10 months. The total electric charge passed through the cell so far exceeds 10$^5$ C/cm$^2$, i.e., 1 mole of electrons per square centimeter. Since about 10$^{-7}$ moles of **1** are adsorbed per square centimeter of projected surface, the sensitizer has sustained

(24) Sakata, T.; Hashimoto, K.; Hiramoto, M. *J. Phys. Chem.* **1990**, *94*, 3040.

(25) Band gap excitation of $TiO_2$ in the presence of organic solvents, such as propylenecarbonate (PC), perturbs the long-term operation of the thin layer cell. Initially the short circuit photocurrent increases while the open circuit photovoltage decreases. The initial phase is over within a few hours of illumination with the full UV output of the 450-W Xe lamp. It is followed by a slower phase during which the current declines below its initial value. The distribution of dye on the $TiO_2$ surface becomes somewhat inhomogeneous; the RuL$_2$(NCS)$_2$ accumulates in certain zones while others are partially depleted. Continued illumination with a 420-nm cut-off filter placed in the light beam sometimes leads to recovery of the initial cell performance. This reversibility rules out that the destruction of the sensitizer is responsble for the observed effects. UV-photoelectrolysis of bare $TiO_2$ films immersed in PC/LiI/LiI$_3$ electrolyte produces a greenish-yellow coloration on the surface of the film. This is due to a weakly adsorbed product arising from the oxidation of the organic solvent by valence band holes, competing with hole capture by iodide. PC scavenges holes to yield an intermediate which subsequently reacts with the iodide/triiodide electrolyte to yield the surface-adsorbed yellowish-green product. This is confirmed by the fact that both the presence of PC and iodide is required for the appearance of the species. Furthermore, its formation is suppressed when water is used as a solvent for the iodine/iodide electrolyte. Photoelectrochemical experiments established that it acts as a charge-transfer sensitizer in the 400–550-nm wavelength domain and at the same time enhances the dark reduction of triiodide by conduction band electrons. This explains the increase in $i_{sc}$ and the decrease in $V_{oc}$ observed in the initial phase during long-term band gap illumination. Accumulation of the hole reaction product at the surface perturbs the adsorption of RuL$_2$(NCS)$_2$ explaining the surface migration of the dye and the photocurrent decrease observed after long illumination times. The reaction of holes with the solvent leads also to depletion of triiodide since the reduction of $I_3^-$ at the counter electrode is not entirely compensated by the concomitant $I_3^-$ regeneration at the photoanode. The depletion of $I_3^-$ is expected to impose diffusion limitations on the cathodic current, and this effect could also contribute to the observed decrease in $i_{sc}$.

(26) Water contamination has an effect on photocell performance, the initial changes in cell performance under visible eight illumination and in the dark are suppressed by using a water-tight cell sealant.

more than $10^7$ turnovers without significant decomposition since the beginning of illumination.

In order to rationalize these observations, we consider the three different states assumed by the sensitizer during redox cycling, i.e., the ground state (S), the oxidized form (S$^+$), and the excited state (S$^*$), the latter being the most unstable species. Reaction channels of S$^*$ are (a) radiative and nonradiative deactivation to the ground state, (b) electron injection into the TiO$_2$ conduction band, and (c) structural changes or decomposition of the electronically excited complex. Few studies exist on the photochemistry of *cis*-Ru(bipy)$_2$X$_2$ complexes (X = Cl, CN, SCN); little is known apart from the fact that these compounds are formed by photosubstitution of Ru(bipy)$_3$ by X.[27-29] Photoinduced *cis–trans* isomerization has been shown to occur.[28,30] However, our previous studies with Ru$^{II}$L$_2$(H$_2$O)$_2$ indicate that this does not lead to deterioration of sensitizer performance.[31] Photoinduced ligand substitution has been observed for *cis*-Ru(bipy)$_2$-(NCS)$_2$ by Hoggard and Porter[29] in dimethylformamide (DMF). When DMF solutions of the complex were irradiated with the full output of a Hg arc lamp, the major product formed was Ru(bipy)$_2$(NCS)(DMF), indicating that replacement of one of the NCS ligands by DMF had occurred. The quantum yield for photosubstitution, $\phi_s$, was estimated to be $7 \times 10^{-4}$. Assuming the same $\phi_s$ value for RuL$_2$(NCS)$_2$, one derives for the rate constant for ligand substitution the value $1 \times 10^4$ s$^{-1}$. This is 1.4 $\times 10^7$ times smaller than the rate constant for charge injection from the excited sensitizer into the conduction band, indicating that after $10^7$ cycles 10% of the complex would have undergone ligand substitution. In agreement with this prediction, we find the UV/vis absorption of sensitizer desorbed from the TiO$_2$ surface after continuous long-term light exposure to exhibit the characteristic feature of RuL$_2$(NCS)$_2$. This excludes that any significant fraction of the complex was converted to the solvent-coordinated species during illumination. Even if such substitution took place over a longer time period, it is unlikely to result in a significant deterioration of cell performance, because substitution of one of the NCS ligands by a coordinating solvent molecule has only a small effect on the absorption spectrum[29] and is unlikely to alter significantly the sensitization efficiency.

Degradation may also occur when the complex is in the oxidized state. Thus, Ru$^{III}$L$_2$(NCS)$_2$ may undergo an internal self-destructive redox reaction involving oxidation of thiocyanate or 2,2'-bipyridyl-4,4'-dicarboxylate by Ru(III). From the reversible nature of the cyclic voltammogram at slow scan rates, it can be inferred that if such a process occurred it would require at least several seconds. This has to be compared with the competing reduction of Ru$^{III}$L$_2$(NCS)$_2$ by iodide, which occurs on a time

scale of $10^{-8}$ s.[32] Again, more than $10^7$ cycles could be sustained in such a case without significant destruction of the complex as is experimentally observed.

## Conclusions

*cis*-X$_2$Bis(2,2'-bipyridyl-4,4'-dicarboxylate)ruthenium(II) complexes (X = Cl, Br, I, CN, and SCN) were prepared and characterized with respect to their absorption, luminescence, and redox behavior. The thiocyanato derivative *cis*-di(thiocyanato)-bis(2,2-bipyridyl-4,4'-dicarboxylate)ruthenium(II) (1) was found to exhibit outstanding properties, taking it a very attractive new redox sensitizer. Of great advantage is its ability to harvest a large fraction of visible light combined with a relatively long excited-state lifetime. This renders it a very useful sensitizer even for homogeneous redox reactions. The four carboxylate groups linked to the two bipyridyl moieties assure intimate adsorption to the surface of oxides such as TiO$_2$, providing at the same time strong electronic coupling between the charge-transfer excited state and the conduction band wave function manifold of the semiconductor. As a consequence, ultrafast electron injection from the excited complex into the semiconductor occurs at near 100% quantum yield.

The potential of 1 as a charge-transfer sensitizer was tested with a recently developed TiO$_2$ film consisting of an array of nanometer-sized particles sintered together by a brief thermal treatment to form a network of interconnected particles of very high surface area. Photoinjected electrons percolate rapidly through the film and are quantitatively collected by the conducting glass support. A thin-layer photoelectrochemical cell based on this system reached a 10% AM 1.5 solar-to-electric conversion yield. This device operates in a regenerative mode: iodide is oxidized to triiodide at the photosensitized TiO$_2$ film, and the latter is reduced back to the original state at the dark counter electrode, eq 6:

$$3I^- \rightarrow I_3^- + 2e^- \text{ (photoanode)}$$
$$I_3^- + 2e^- \rightarrow 3I^- \text{ (dark cathode)} \tag{7}$$
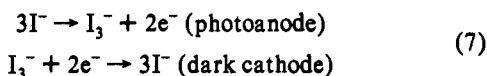
There is no net chemical change associated with the functioning of the cell which converts light to electricity. For the first time, a device based on a simple molecular light absorber attained an efficiency commensurate with that of conventional photovoltaic cells.

(27) Gleria, M.; Minto, F.; Beggiato, G.; Bortulus, P. *J. Chem. Soc., Chem. Commun.* **1978**, 285.

(28) Durham, B.; Caspar, J.; Nagle, J. K.; Meyer, T. J. *J. Am. Chem. Soc.* **1982**, *104*, 4803.

(29) Hoggard, P. E.; Porter, G. B. *J. Am. Chem. Soc.* **1978**, *100*, 1457.

(30) Walsh, J. L.; Druham, B. *Inorg. Chem.* **1982**, *21*, 229.

(31) Nazeeruddin, M. K.; Liska, P.; Moser, J.; Vlachopoulos, N.; Grätzel, M. *Helv. Chim. Acta* **1990**, *73*, 1788.

(32) The rate of recycling of the dye by reaction with iodide was derived from time-resolved laser photolysis experiments as described in ref 12.